

Hybrid pedestrian and transit priority zoning policies in an urban street network: Evaluating network traffic flow impacts with analytical approximation

Nicholas Fournier, PhD

*Institute of Transportation Studies,
University of California, Berkeley
409 McLaughlin Hall, Berkeley, California 94720*

Abstract

Pedestrianized zones are becoming an increasingly popular policy tool for cities seeking to improve “walkability”, “livability”, and reduce congestion in the urban center by prohibiting automobiles from entering a designated zone. However, pedestrianized zones can be inappropriately implemented in locations without justifiable congestion or sufficient transit alternatives. For mixed-traffic transit (e.g., bus and light-rail streetcars), the lack of reasonable transit alternatives is an issue further compounded by the traffic congestion generated from diverted driving trips concentrated around the pedestrianized zone, inadvertently slowing down both automobile traffic and mixed-traffic transit in tandem. Alternatively, to mitigate the traffic congestion impact on transit, policy makers can also designate a “transit priority” zone around the pedestrian zone, where transit is unimpeded by congestion either through transit signal priority, dedicated lanes, or both. This ensures transit provides a consistent travel alternative as congestion varies, creating a stable demand equilibrium that would otherwise be suppressed by congestion. While such a solution has been proposed in advocacy, no research has explored such a combined policy in analytical terms. This research explores the potential complementary benefits and optimal sizing of pedestrianization and transit priority zones through analytical evaluation in an idealized rectilinear city. The model is intended to provide insights regarding traffic impacts, optimal zone sizing, system capacity, and the justifiable thresholds for implementing complementary pedestrianization and transit priority zones in a city.

Keywords: transit priority, pedestrianization, pedestrian only zone, policy

¹ 1. Introduction

² Congestion, particularly automobile congestion, is often seen as the persistent foe of economic
³ efficiency in dense urban cities [1–7]. For decades, planners and engineers have sought to mitigate
⁴ this endemic issue of congestion through road capacity expansion and urban density controls (i.e.,
⁵ land use zoning policies). However, this often comes at the demise of historic urban centers, and
⁶ more recently, an affordable housing shortage due to a constrained supply of low-density single-
⁷ family dwelling only zoning. In an effort to reverse this trend, planners and politicians occasionally
⁸ implement pedestrian only zones as a particularly aggressive and dogmatic approach to urbanism.
⁹ Pedestrian zones function by severely limiting or prohibiting automobile traffic in an area or corridor
¹⁰ of a city, thereby enforcing walkability.

¹¹ Pedestrian zone policies have and continue to be implemented, but these experimental policies
¹² too often fail to achieve the desired results due to inadequate supporting conditions. One such
¹³ condition is providing reasonable transportation alternatives (i.e., transit). Otherwise pedestrian
¹⁴ zones could fail to attract people, or worse, end up causing more congestion as diverted routes are

concentrated around the zone. Furthermore, with the bulk of transit systems operating in mixed-traffic (e.g., buses or light-rail sharing lanes with traffic), the congestion compounds the problem by further slowing transit even if transit does exist.

Another related policy is “transit priority”, which holds a potential solution. Transit priority is often broadly defined as any policy, infrastructure, or operational strategy that gives transit priority over automobile traffic. There exists a spectrum of strategies, from signal timing to physical infrastructure, that can be used to provide some level of priority. Often, transit priority is simply a signal control strategy which provides some advantage to transit vehicles (e.g., red truncation, green extension, and progressive signal coordination), with little or no change to physical road geometry. This type of transit priority will be referred to as “transit *signal* priority”. While transit signal priority is a relatively new technology in practice, the concept itself has been experimented with since at least the 1970s [8, 9]. Although transit signal priority can provide some advantage to transit vehicles through various control strategies, effectiveness is still ultimately limited by road capacity and mixed-traffic congestion.

A more aggressive transit priority approach is to provide a physically dedicated right-of-way (e.g., bus only lane, elevated rail, or subways) which limits or restricts private vehicle traffic. In the case of bus only lanes or Bus Rapid Transit (BRT), this ensures transit vehicles are unimpeded by congestion, offering rail-like service reliability at a fraction of the cost. Unfortunately, transit priority generally comes at high cost (e.g., rail) or the loss of valuable road space and capacity (e.g., bus only lanes taking a traffic or parking lane) and is seldom politically popular [10]. However, where the political will exists to implement pedestrian zones, transit priority is a modest extension but holds enormous complementary benefits and is ideally suited to mitigating the possible shortcomings of pedestrianization policies. Moreover, by ensuring that transit operates unimpeded, it provides a demand stabilizing effect. As automobile congestion and travel time rise, a reliable transit alternative becomes a more attractive mode choice, creating a stable demand equilibrium and preventing demand from being suppressed by high travel times due to congestion [11–14].

This notion of suppressed demand is also important when considering other policy levers for travel demand management, such as pricing (e.g., transit fares, tolls, congestion pricing, parking pricing, etc.). Imposing pricing policies offers an effective means of controlling travel demand and moving towards a more effective equilibrium point without major infrastructure investment [15–23]. However, without any reasonable travel alternatives, such as transit, demand will simply be suppressed. This may alleviate congestion, but does little to support economic activity or personal mobility and accessibility.

In an effort to preserve or revitalize urban centers and reduce congestion, pedestrian zones and transit priority are two increasingly popular planning policy tools. However, neither pedestrianization nor transit priority are new concepts, urban planners and community activists have been advocating for more “walkable” [24–26] and “transit oriented” [27, 28] urban environments for decades. This paper will, however, not delve into vast philosophy of urban theory and planning existentialism. The purpose is more narrowly focused on travel time reduction through the complementary benefits of pedestrianized zones and transit priority. However, it is important to equip the reader with the background understanding of “urbanism” to explain why cities might seek to reverse their automobile dependence.

While there have been numerous studies and books published highlighting the potential social, environmental, and economic benefits of walkability and pedestrian-centric design, these studies often lack an objective and quantitative evaluation to justify their claims. Conversely, there have been a multitude of technologically driven engineering research on transit signal priority [29–31] and optimization [32–34], but are too narrowly focused site-specific performance to realize the greater systemic benefits if broadly implemented in a city, let alone with pedestrianization [35–37]. This research aims to bridge the gap between planning and engineering by modeling the combined effect of pedestrianized and transit priority zones in an analytical model of an idealized city in order to explore the possible outcomes.

66 To many “traditional” traffic engineers, pedestrianization and transit priority may appear as
67 radical, inefficient, and directly in opposition to their efforts to provide an efficient transportation
68 system for the modern economy. But it is important to consider the broader contextual motivation
69 of such policies; that is, to create urban environments for people in cities, not their automobiles.
70 Traffic engineers are not necessarily wrong, many pedestrian oriented concepts are loose abstract
71 philosophies, lacking tangible and objective solutions for the modern world. This paper seeks to help
72 remedy this by providing a mathematical analysis of a pedestrianized zone surrounded by transit
73 priority. The problem is simplified for an idealized city with a rectilinear grid street network in order
74 to explore a range of outcomes. The purpose of this paper is to not only provide a model, but to
75 demonstrate the complementary benefits of such policies in a generalized and objective form.

76 *1.1. Modeling philosophies*

77 Among academics, there is often a muted tension between idealized analytical modeling approaches and empirical models. Analytical models are theoretical approaches using continuous
78 mathematical approximations based on physical and geometric properties, often applied to represent
79 static traffic equilibrium or transit network operations and explore hypothetical outcomes
80 [38–45]. While analytical approaches offer elegant solutions, more complex problems are not easily
81 solved, such as traffic assignment and dynamic mode-choice, requiring stochastic or deterministic
82 numeric solutions [46–50]. Prior to the proliferation of high-powered computation over the last few
83 decades, classical analytical models largely dominated. Since then, the field has given way to more
84 data driven discrete choice, simulation models, and more recently, artificial intelligence capable of
85 high-resolution predictions far beyond simplistic analytical models [51–56].

86 Analytical models are often rightfully criticized as being overly simplified and hyper-idealized
87 cases with little or no practical application outside of academic text. While true that simulation’s
88 precision offers abundant practical applications (e.g., travel demand models and system optimization),
89 they are often immensely sophisticated “black-box” estimations, rely on past data, and too
90 frequently validated against other simulated results. This obscures any broad functional systemic
91 relationships that might exist and limits simulation results only to where sufficient explanatory data
92 exists; and not with, for example, untested pedestrianized and transit priority zones. Analytical
93 models in contrast, focus primarily on those functional relationships, helping shed broader insight
94 for policy that can then later be refined through simulation.

95 The following analytical model is not meant to provide high-resolution results, nor is it meant to
96 provide a grand unifying mathematical function. It is merely intended to demonstrate in quantitative
97 terms, the potential complementary benefits of pedestrianized zones surrounded by transit priority.
98 The goal is that a simplified, objective, and unbiased model might help dissolve some of the opinions
99 and misguided advocacy that might lead to an impractical or inappropriate policy decisions. Of
100 course, this model is hyper-idealized, only measures travel time, and does not account for the
101 multitude of other social and economic factors beyond basic commuter behavior. It is possible that
102 if the results were implemented in broad strokes, as was done with the automobile oriented boom
103 of the 20th century, there would most likely be numerous unexpected negative side effects. The
104 results should not be taken as cause to radically rebuild, but to help better understand the potential
105 benefits that pedestrianization and transit priority have in increasing system capacity and reducing
106 travel times.

108 **2. Concept**

109 Consider an idealized city of dimension R with rectilinear street network with spacing d , as
110 shown in Figure 1. Demand can be defined by two types of trip patterns, baseline uniform travel
111 demand across the city and monocentric trips to and from the city center. The cumulative effect
112 is increased congestion in the city center. To make the city center more attractive, “livable”, and
113 “walkable”, policy makers designated a square pedestrianized zone of size γ in the city center,

114 allowing only pedestrians, bicycles, and transit vehicles. The pedestrianized zone forces drivers
 115 entering the center of the city to park at the perimeter and walk, possibly increasing travel time.
 116 This increased travel time potential makes transit more attractive if transit can still enter the
 117 pedestrianized zone. However, the pedestrianized zone forces drivers to divert routes around the
 118 zone, increasing traffic density and congestion as a result. To mitigate the traffic congestion impact
 119 on transit (e.g., buses and streetcars/trams), policy makers also designated a “transit priority” area
 120 of dimension τ , around the pedestrian zone, where transit is unimpeded by congestion either through
 121 transit signal priority, dedicated right-of-way (e.g., bus only lane, elevated track, or subways), or
 122 both .

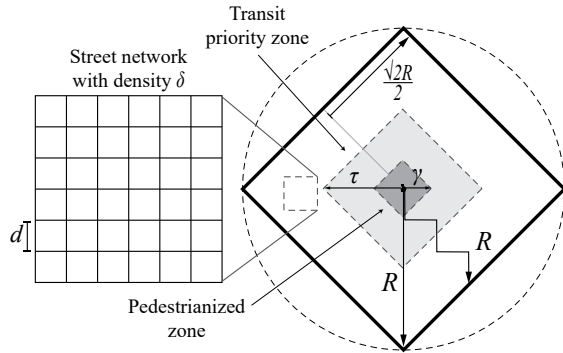


Figure 1: Rectilinear city with pedestrianized zone

123 Typically, transit priority is not conceptualized as a zone. In practice, transit priority is typ-
 124 ically implemented along designated radial corridors leading towards the city center. However, at
 125 a macroscopic regional scale, transit priority generally falls within a central region of a city where
 126 traffic congestion is severe enough to justifies transit priority. Thus, in this conceptualization it is
 127 not necessarily that every street within the transit priority zone has transit priority, but the transit
 128 corridors in the zone are unimpeded by transit.

129 2.1. Mode choice

130 Mode choice in this model is fundamentally a binary choice between driving and transit.
 131 However, if their destination is located within the pedestrianized zone, they can either take transit
 132 for the entire trip or drive to the perimeter and walk the remaining distance within the pedestrianized
 133 zone. The decision criterion is assumed to be based on travel time. Although travel time is a major
 134 factor affecting mode choice, it is important to note that in reality it is only one among many factors
 135 (e.g., safety, comfort, accessibility, cargo, etc.) [57, 58]. For simplicity, this model assumes that mode
 136 choice depends entirely on travel time, meaning that travelers choose whichever mode provides the
 137 shortest travel time. However, future extensions of this model could partially account for biases or
 138 other “utilities” by weighting the travel times associated with each mode.

139 Assuming that driving and mixed-traffic transit are delayed by automobile congestion but trans-
 140 it priority and pedestrians are not, then it may be possible to manipulate travel time and demand
 141 through complementary pedestrian and transit priority zoning policies, described in Figure 1. Con-
 142 gestion in the city center may be eliminated by imposing a pedestrianized zone, forcing drivers to
 143 walk the remaining distance. This may forcibly eliminate congestion in the city center, but sizing of
 144 the pedestrian zone is critical as any reduction in congestion delay may be quickly outweighed by
 145 perimeter road congestion and the additional time spent walking if the zone is too large. For transit
 146 priority, its stable travel time becomes more attractive as driving demand and congestion increase.
 147 However, assuming transit cannot exceed the speed of automobiles (i.e., there is a speed limit),
 148 then there is no benefit to providing transit priority beyond where congestion exists in the city.

149 Conversely, if no transit priority exists, then transit will always be slower than driving due to stops
 150 and dwell time, offering little incentive for drivers to change modes. Based on these assumptions,
 151 a model can be formulated to minimize travel time by manipulating the size a pedestrianized zone
 152 and transit priority zone, finding an optimal size of both.

153 *2.2. Objective*

154 The objective of this conceptual model is to minimize average total travel time for travelers in
 155 the city by determining the optimal pedestrian only and transit priority zone sizes. While both the
 156 pedestrian only and transit priority zone ultimately contribute to the primary objective of reducing
 157 average total travel time, they both have their own individual objectives and constraints. The
 158 pedestrian zone on its own has the objective of preventing traffic flow from exceeding capacity in the
 159 city center. The transit priority zone is then subsequently implemented to mitigate any increased
 160 travel time due to excess walking distance or traffic generated by the pedestrianized zone. The goal
 161 in this paper is to reduce the two problems such that they share the same parameters and can be
 162 evaluated in single unified objective function accounting for both policies simultaneously. There are
 163 three basic components necessary to build and evaluate the conceptual model:

- 164 1. Travel demand – the number of trips and their flow direction.
 165 2. Travel distance – the average trip distance per mode.
 166 3. Travel time – the average travel time per mode which depends upon demand-based congestion.

167 From these three components, the average total travel time can then be calculated and evaluated.
 168 The following subsections will discuss the necessary components in further detail.

169 *2.3. Travel demand*

170 Demand is generated in the city area in units of $\frac{\text{trips}}{\text{dist}^2 \cdot \text{time}}$, and can be simplified into two types:
 171 • uniform baseline travel across the network, λ_b , and
 172 • monocentric travel demand going to and from the centroid of the city, λ_c .

173 Average trip flow can be calculated as the product of trip demand and average trip length,
 174 divided by the amount of roadway infrastructure available to carry these trips, yielding trip flow
 175 in units of $\frac{\text{trips}}{\text{lane} \cdot \text{time}}$. Thus, the baseline traffic flows (see Figure 2a) associated with average trip
 176 length¹, l_b , generate $q_b = \frac{\lambda_b l_b}{\delta}$ flow across the network, where δ is the roadway network density² in
 177 units of $\frac{\text{lane} \cdot \text{dist}}{\text{dist}^2}$. There is then the additional traffic flow associated with monocentric trips to and
 178 from the center that varies with the distance from the center (see Figure 2b). Consider a square of
 179 infinitesimal perimeter width dr , at distance r from the center, the total demand for trips crossing
 180 this square is $2\lambda_c(R^2 - r^2)$. The trips generated by this demand then travel a distance dr across the
 181 square using the available road infrastructure of $4\sqrt{2}r\delta$.

¹The average baseline distance, l_b can be calculated from the expected Manhattan distance distributed across a unit square, $E(D) = \iint \iint \frac{1}{4}(|x_1 - x_2| + |y_1 - y_2|) dy_2 dx_2 dy_1 dx_1$ with the limits of $-R \leq x_1 \leq R$, $|x_1| - 1 \leq y_1 \leq 1 - |x_1|$, $-1 \leq x_2 \leq 1$, and $|x_1| - 1 \leq y_2 \leq 1 - |x_1|$. Since $|x_1 + x_2|$ and $|y_1 + y_2|$ are identical, it can be simplified to $2 \int_{-1}^1 \int_{-1}^1 |x_1 - x_2|(1 - |x_1|)(1 - |x_2|) dx_2 dx_1$, which evaluates to $\frac{14}{15}$ as proportional to any size R , thus $l_b = \frac{14}{15}R$. The average monocentric Manhattan distance, l_c , to the center of the square is equivalent to the Euclidean distance to the center in a circle of size R , thus the average expected distance is $l_c = \frac{2}{3}R$ [59]. The overall average travel distance is then $l = \frac{R(14\lambda_b + 10\lambda_c)}{15(\lambda_b + \lambda_c)}$.

²The calculation for network density can be derived as the total roadway length $2n(n+1)d$, divided by total area nd^2 ; both of which can be expressed as a function of the number of city blocks n , and the street spacing dimension d . The relationship between δ and d is linearly constant, yielding $\delta = \frac{2}{d}$.

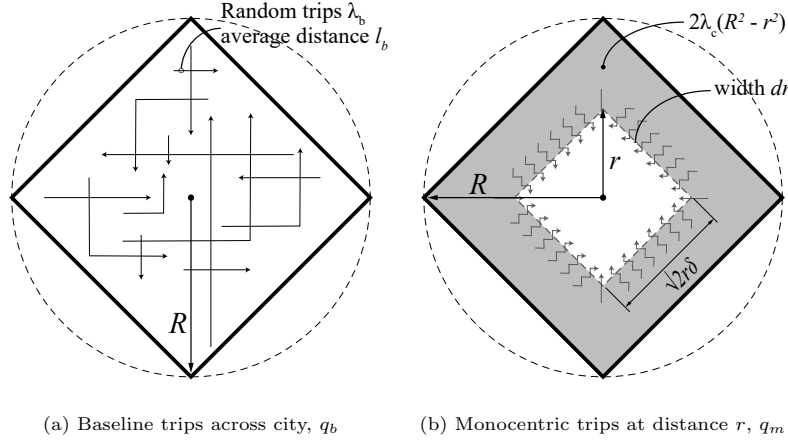


Figure 2: Baseline and monocentric trip diagram

182 The average monocentric flow through the network at a point with a distance r from the city
 183 center is then $q_m(r) = \frac{2\lambda_c(R^2 - r^2)}{4\sqrt{2}\delta r}$. The combined flow at distance r from the city center is then the
 184 combined sum, calculated as:

$$q_a(r) = \frac{14R\lambda_b}{15\delta} + \frac{\lambda_c}{2\sqrt{2}\delta r} (R^2 - r^2) \quad (1)$$

185 The pedestrianized zone will cause some trips to be diverted around the pedestrian zone along a
 186 square perimeter zone created by the “pinch points” at the corners. Assuming travelers choose the
 187 shortest route, but will choose an available equidistant route to avoid congestion, trips in the city
 188 can be categorized into four distinct types (see Figure 3):

- 189 1. Unimodal routes entirely within the pedestrianized zone that are unaffected by congestion,
- 190 2. Bimodal routes taking vehicles to perimeter of pedestrianized zone to park nearest the desti-
 191 nation and the remaining radial distance is traveled on foot,
- 192 3. Unimodal routes entirely outside the pedestrianized zone that can avoid congestion created by
 193 the zone, and
- 194 4. Unimodal routes that would have passed through the center, whose shortest paths are now
 195 diverted to the “pinch points” created by the pedestrianized zone vertically and horizontally.

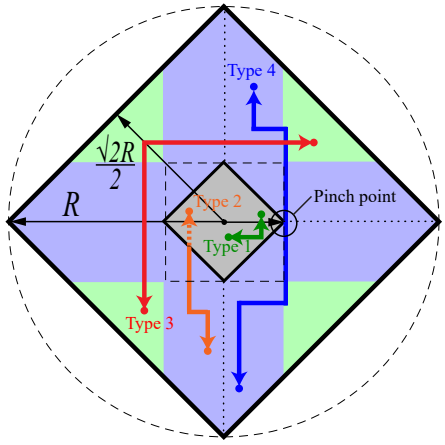


Figure 3: Example diverted route types

In a rectilinear grid, multiple equidistant paths exist that can be used to avoid congestion. Trip types 2 and 3 can avoid traveling along the pinch point perimeter by taking an earlier or later turn without increasing distance. However, trip type 4 cannot avoid the pinch point perimeter unless extra turning movements or a longer path is taken. While a longer route can and will be chosen in reality, the worst case is assumed that travelers will choose the shortest path and face congestion at these pinch point perimeter roads. To determine the trip flow along this perimeter, the shaded areas in Figure 3 denote the contributing demand area for each trip type. The expected trip flow (vehicle-distance/time) on the perimeter road is the product of three values: the number of trips originating in the critical city half between γ and R , $\lambda_b(R^2 - \gamma^2)$; the probability that a trip destination falls within the trip category, $\frac{\gamma(R-\gamma)}{R^2}$; and the expected distance per trip on the pinch point perimeter road, 2γ . Dividing the total in $\frac{\text{trips} \cdot \text{dist}}{\text{time}}$ by the length of the perimeter traversed³, 2γ , provides the critical flow in $\frac{\text{trips}}{\text{time}}$ on the perimeter road:

$$q_p(\gamma) = \frac{\lambda_b \gamma (R - \gamma)(R^2 - \gamma^2)}{R^2} \quad (2)$$

The trip demand flow density across the network at distance r from the city center, from the function in Equation (1), possesses the form shown in Figure 4a. As the distance from the city increases, traffic decreases. When traffic near the center exceeds capacity, one might consider simply pedestrianizing the city center out to the point where capacity is no longer exceeded. However, as more trips are diverted around the perimeter zone, traffic congestion on the perimeter road can increase as the zone size increases. The trip demand flow around the perimeter of the pedestrian zone, from Equation (2), possesses a parabolic-like shape with a long-tailed right side, shown in Figure 4b.

An interesting note is that the long-tailed parabolic-like form is unique to rectilinear grids. A ring-radial street network yields a half parabola-like form centered at the origin so that a non-zero pedestrianized zone starts with the maximum traffic, then rapidly improving at an accelerating rate [60]. The reason for this is not immediately apparent, but makes intuitive sense when considering possible route alternatives in each network structure.

As a pedestrianized zone in a rectilinear grid increases in size, it causes a larger number of trips to be diverted around the perimeter, increasing perimeter road traffic. However, once the pedestrianized zone becomes so large, a majority of trips are entirely contained within the pedestrianized zone,

³It is conservatively assumed that travelers traverse the entire perimeter edge to avoid extra turning movements.

causing perimeter road traffic to decrease. Somewhat counter-intuitively in a ring-radial city, the traffic congestion is worst for the smallest non-zero pedestrianized zone. This is because, unlike in a rectilinear grid, there are no equidistant alternative routes around the perimeter road, making the perimeter route the shortest route. In reality it is more likely that traffic congestion in the ring-radial network will find some equilibrium flow distributed across the network, rather than concentrate along one route. However, urban road networks are seldom ever a geometrically perfect rectilinear grid or ring-radial structure, and may even be some combination of the two.

In either case, the pedestrianized zone may eliminate congestion in the city center, but would greatly increase travel time by walking. An appropriate policy might try to find a balance between where the city center is pedestrianized enough to reduce congestion in the center, but not too much to create perimeter road congestion.

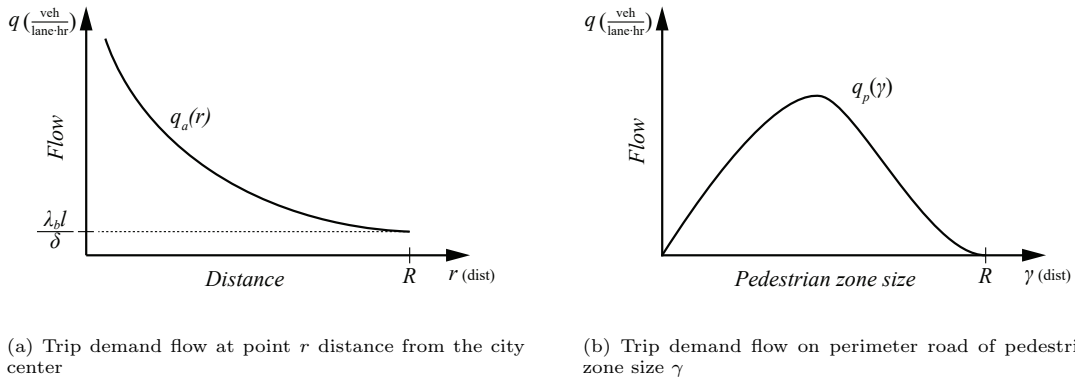


Figure 4: Trip demand flow

2.4. Travel distance

To determine the travel time, the total average distance traveled must be calculated for each travel mode. The average travel distance for driving, pedestrians, and transit are described in the following sub-sections.

2.4.1. Average driving distance

The driving distance is the average driving distance for baseline trips ($\frac{14}{15}(R - \gamma) \times \frac{\lambda_b}{\lambda_b + \lambda_c}$) and monocentric trips ($\frac{2}{3}(R - \gamma) \times \frac{\lambda_c}{\lambda_b + \lambda_c}$) outside of the pedestrian zone, multiplied by the proportion of respective trip demand. The combined function can be simplified to

$$l_D = \frac{(R - \gamma)(14\lambda_b + 10\lambda_c)}{15(\lambda_b + \lambda_c)} \quad (3)$$

2.4.2. Average pedestrian distance

Pedestrian trips are also generated by the baseline demand (b) and the monocentric central demand (c). Let D_{ij} be demand amount and l_{ij} be the average walking distance covered in each case ij where i is trip types {1, 2} and j is demand type {b, c}. The total distance covered within the pedestrianized zone l_P is then:

$$l_P = \frac{\sum_{i,j} D_{ij} l_{ij}}{\sum_{i,j} D_{ij}} \quad (4)$$

where:

- 249 • $D_{1b} = 2\lambda_b\gamma^2 \times \frac{\gamma^2}{R^2}$: Total baseline demand trips originating in pedestrian zone by the proportion
 250 ending in the pedestrian zone.
- 251 • $D_{2b} = 4\lambda_b(R^2 - \gamma^2) \times \frac{\gamma^2}{R^2}$: Total baseline demand trips originating inside and ending outside
 252 the pedestrian zone, and vice versa. Both cases equal $2\lambda_b(R^2 - \gamma^2) \times \frac{\gamma^2}{R^2}$.
- 253 • $D_{1c} = 2\lambda_c\gamma^2$: Total monocentric trips originating inside the pedestrian zone.
- 254 • $D_{2c} = 2\lambda_c(R^2 - \gamma^2)$: Total monocentric trips originating outside the pedestrian zone.
- 255 • $l_{1b} = \frac{14}{15}\gamma$: Average distance of baseline trips that originate and end in the pedestrian zone.
- 256 • $l_{2b} = \gamma$: Average distance of baseline trips that originate from the pedestrian zone perimeter
 257 (i.e., the point where traveler changes mode to walk) to some uniformly distributed destination
 258 in the zone.
- 259 • $l_{1c} = \frac{2}{3}\gamma$: Average distance of monocentric trips that originate and end in the pedestrian
 260 zone.
- 261 • $l_{2c} = \gamma$: Average distance of monocentric trips that originate from the pedestrian zone
 262 perimeter to the city center.

263 The combined function then becomes:

$$l_P = \frac{-32\lambda_b\gamma^5 + (60\lambda_b + 5\lambda_c)R^2\gamma^3 + 15R^4\lambda_c\gamma}{15(4\lambda_bR^2\gamma^2 - 2\lambda_b\gamma^4 + 2R^4\lambda_c)} \quad (5)$$

264 2.4.3. Average transit distance

265 Transit distance must be separated by the portion traveled in transit priority and in mixed traffic
 266 to calculate the appropriate travel time:

- 267 • In mixed traffic it is the average distance traveled outside the priority zone:

$$l_{TM} = \frac{(R - \tau)(14\lambda_b + 10\lambda_c)}{15(\lambda_b + \lambda_c)} \quad (6)$$

- 268 • In transit priority it is the average distance traveled inside the priority zone:

$$l_{TP} = \frac{\tau(14\lambda_b + 10\lambda_c)}{15(\lambda_b + \lambda_c)} \quad (7)$$

269 2.5. Travel time

270 The average total travel time is calculated using the respective travel time functions for each
 271 mode type and demand split:

$$\bar{t}_{total}(\gamma, \tau) = \Phi_D(\tau) \times \left(\bar{t}_D(\gamma) + \bar{t}_P(\gamma) \right) + \left(1 - \Phi_D(\tau) \right) \times \left(\bar{t}_{TP}(\tau) + \bar{t}_{TM}(\tau) \right) \quad (8)$$

272 where $\bar{t}_{total}(\gamma, \tau)$ is the average total travel time, $\bar{t}_D(\gamma)$ is the average driving travel time, $\bar{t}_P(\gamma)$
 273 is average travel time within the pedestrianized zone, $\bar{t}_{TP}(\tau)$ is the average transit priority travel
 274 time, $\bar{t}_{TM}(\tau)$ is the average mixed-traffic transit travel time, and $\Phi_D(\tau)$ is the proportion of trips
 275 driven by car. These travel times are calculated using the respective travel demand and distances
 276 described in previous sections. However, in addition to this travel time, delay due to congestion will
 277 be experienced for driving and mixed-traffic transit. This congested travel time will be discussed in
 278 the following subsections.

279 2.5.1. *Traffic flow*

280 Congested travel time (i.e., driving and mixed traffic transit) depends upon the state of traffic
 281 flow through the network. Traffic flow through the network can be characterized by the macroscopic
 282 fundamental diagram (see Figure 5a) as a function of trip demand density [61–64]. A travel time
 283 function (see Figure 5b) then depends upon the state of traffic flow through the network as being
 284 either “uncongested” (solid line) or “congested” (dashed line) in Figures 5a and 5b.⁴

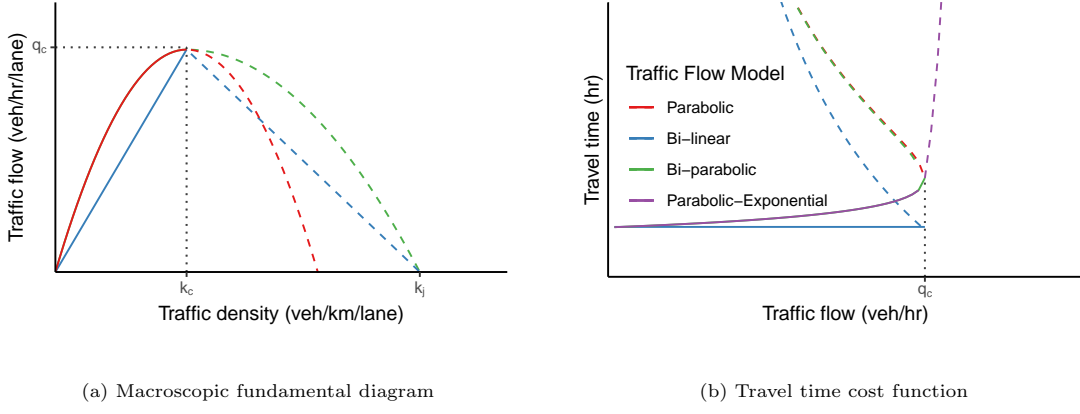


Figure 5: Macroscopic fundamental diagram and travel time cost function

285 Although a variety of more refined macroscopic models have been developed, many are often
 286 very sophisticated and require additional calibration parameters, or possess abrupt transitions that
 287 can create anomalies in analytical results. Two common classical models that require no additional
 288 calibration parameters are Greenshields’ [67] parabolic function and Daganzo’s [68] bi-linear model.
 289 Greenshields’ seminal function is elegantly simple, but symmetric parabolic shape has since been
 290 proven a poor fit in reality, particularly when critical density, k_c , is exceeded. Daganzo’s model
 291 in contrast provides a very simple parsimonious model with an asymmetric form, but its linearity
 292 assumes a constant free-flow speed until it abruptly transitions at critical density. The constant free-
 293 flow speed not only ignores minor delay caused by gradual slowing of traffic as density increases,
 294 but causes an abrupt transition that can cause erroneous results with the sudden jump.

295 Assuming for this case a parabolic function represents the uncongested portion of the flow-density
 296 relationship, an expression for the “uncongested” solid line portion of Figure 5a can be written as:

$$q(k) = q_c \frac{k(2k_c - k)}{k_c^2} \quad (9)$$

297 where k_c is the density at capacity, and q_c is the flow at capacity. In order to determine travel time,
 298 density as a function of flow $k(q)$ can be solved as a quadratic:

$$k(q) = k_c \left(1 - \sqrt{1 - \frac{q}{q_c}} \right) \quad (10)$$

299 However, a problem in calculating travel time using the macroscopic fundamental diagram is its
 300 concave form which results in a backward bending travel time function once trip demand exceeds
 301 capacity [65]. From this flow-density, a piece-wise monotonic cost function for travel time, as shown
 302 in Figure 5b, can then be defined as:

⁴Literature has also classified these two states as “congestion” and “hypercongestion”, where any traffic density affecting traffic speed (i.e., any density $k > 0$) is considered “congested” and when capacity is exceeded (i.e., when density $k \geq k_c$) it is “hypercongested” [65, 66].

$$t(q) = \begin{cases} q < q_c : & l \frac{k(q)}{q} \\ q \geq q_c : & t_c \left(\frac{q}{q_c} \right)^{20} = l \frac{k_c}{q_c} \left(\frac{q}{q_c} \right)^{20} \end{cases} \quad (11)$$

303 where $t(q)$ is travel time for flow q , $k(q)$ is traffic density for flow q , l is link length, q_c is link
 304 capacity, and $t_c = l \frac{k_c}{q_c}$ is the travel time at capacity. The congested portion for travel time can
 305 be simply modeled as a sufficiently steep monotonically increasing function. To avoid an abrupt
 306 transition from the uncongested portion, a very high exponent of 20 was chosen to closely match the
 307 parabolic function's trajectory without being perfectly vertical. This provides a smooth transition
 308 from parabolic to exponential. The average travel time in traffic \bar{t} , can be determined from the
 309 average travel distance \bar{l} , divided by average speed \bar{v} :

$$\bar{t} = \frac{\bar{l}}{\bar{v}} = \bar{l} \frac{k(\bar{q}_a)}{\bar{q}_a} \quad (12)$$

310 which can be analytically determined from the macroscopic fundamental diagram as a function
 311 of average flow across the network \bar{q}_a , as experienced by travelers from their trips between the
 312 pedestrian zone γ , and the city limit R :

$$\begin{aligned} \bar{q}_a &= \frac{1}{R - \gamma} \int_{\gamma}^R q(\gamma) d\gamma \\ \bar{q}_a &= \frac{14R\lambda_b}{15\delta} + \frac{\lambda_c}{8\delta(R - \gamma)} \left[2R^2 \ln \left(\frac{R}{\gamma} \right) + \gamma^2 - R^2 \right] \end{aligned} \quad (13)$$

313 which can then be used to determine the average travel time in traffic.

314 2.5.2. Transit

315 Transit travel time is conditional upon whether it operates in a transit priority zone (e.g., dedicated
 316 lane or right-of-way) or in mixed-traffic (e.g., city bus). In transit priority it is assumed there
 317 is no other source of delay other than delay due to stopping, which can be calculated from the
 318 average lost time from stopping, t_s , and the stop spacing, s . In mixed traffic the transit travel time
 319 is this stopping delay plus delay from congestion. These travel times can be calculated as:

$$t_{TP} = \frac{l}{v_m} + \frac{l}{s} t_s \quad \text{with transit priority} \quad (14a)$$

$$t_{TM}(q) = l \frac{k(q)}{q} + \frac{l}{s} t_s \quad \text{without transit priority when } q < q_c \quad (14b)$$

$$t_{TM}(q) = l \frac{k_c}{q_c} \left(\frac{q}{q_c} \right)^{20} + \frac{l}{s} t_s \quad \text{without transit priority when } q \geq q_c \quad (14c)$$

320 where v_m is the maximum cruising speed of transit unimpeded by traffic. The stop time is essentially
 321 the lost time inclusive of acceleration, deceleration and dwell time. The travel time of transit in
 322 mixed-traffic will then always be higher than driving an automobile. A similar observation was
 323 also found by Geroliminis et al. [69] using a bi-modal three-dimensional macroscopic fundamental
 324 diagram. In this model, the travel times will eventually converge as traffic conditions reach jam
 325 flow. Conversely, transit priority provides a constant travel time which will be initially slower than
 326 driving in uncongested traffic conditions, but will eventually reach a traffic flow point q_T , where the
 327 travel time of transit with priority exceeds driving (see Figure 6).

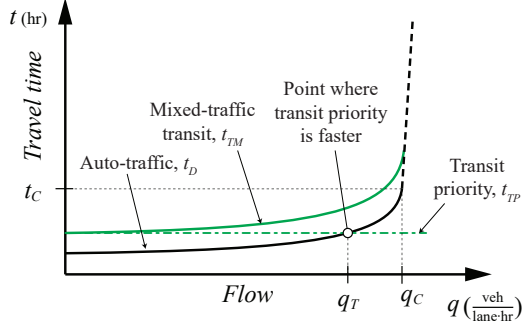


Figure 6: Driving and transit travel time

329 The critical transit priority traffic flow point q_T , is found where transit priority travel time t_{TP}
 330 intersects driving travel time t_D . Since travel time is a piece-wise function, it depends on whether the
 331 transit priority travel time t_{TP} , exceeds the driving travel time at roadway capacity t_c . Although it is
 332 unlikely that transit priority travel time will exceed this point, the condition is provided nonetheless.
 333 To determine when this occurs, a simple ratio can be taken, t_{TP}/t_c . The critical transit priority traffic
 334 flow point then depends on whether t_{TP}/t_c is greater than or less than 1:

$$q_T = \frac{2k_c}{T} - \frac{k_c^2}{q_c T^2} \quad \text{for } t_{TP}/t_c < 1 \quad (15a)$$

$$q_T = q_c \left(\frac{q_c}{k_c} T \right)^{\frac{1}{20}} \quad \text{for } t_{TP}/t_c \geq 1 \quad (15b)$$

(15c)

where:

$$T = \frac{1}{v_m} + \frac{t_s}{s}$$

$$t_{TP}/t_c = \frac{q_c}{k_c} \left(\frac{1}{v_m} + \frac{t_s}{s} \right)$$

335 For simplicity, it is assumed that transit priority does not affect driving in this model. In reality
 336 it is possible that transit and transit priority may affect driving conditions. For example, if a driving
 337 lane is taken from cars to create a dedicated bus lane or if bus traffic is high enough to congest overall
 338 traffic. However, it is possible that “transit priority” could be designed or constructed to minimize
 339 or avoid any impact on driving conditions. For example, some signalization strategies that gives
 340 transit priority with minimal traffic impacts, or a separate transit right-of-way was added that does
 341 not take away from driving lanes. An example of this would be an elevated track or underground
 342 subway, a form of “transit priority” that has existed for centuries. Nonetheless, it should be stated
 343 that transit priority can impact driving conditions but is not accounted for in this model.

344 As stated, many assumptions are used to make this model tractable and parsimonious. However,
 345 it may be possible to better account for the effects of mixed-traffic transit using more sophisticated
 346 models. There exists a growing body of research that extends the macroscopic fundamental diagram
 347 to include an additional dimension for transit vehicles [69–71]. These models begin to dissect the
 348 vehicle fleet in the traffic flow, so that the relative proportion of buses and automobiles can account
 349 for the different, yet combined effect of a mixed-traffic flow. This multidimensional stratification
 350 enables details for the respective modes to be better understood, and even optimized using one
 351 unified model, the macroscopic fundamental diagram [72, 73]. However, the added complexity of a

352 multi-dimensional model makes the objective in this problem, to determine the optimal pedestrian
 353 and transit zone sizes, far more difficult to solve. Future work could investigate this area of research.

354 **3. Zone sizing**

355 There are two zones that require sizing, the pedestrian only zone and the transit priority zone.
 356 The two zones have varying goals but which can work simultaneously to improve travel flow across
 357 the city holistically. The pedestrian zone is concerned with preventing traffic flow from exceeding
 358 roadway network capacity in the center. However, the zone cannot be too large as to cause perimeter
 359 road traffic to exceed capacity or to cause travel times to increase due to walking. Thus, transit
 360 priority is then concerned with mitigating excess congestion around the pedestrianized zone by
 361 providing a stable travel alternative. The sizing of the pedestrianized zone and transit priority zone
 362 are described in more detail in the following two subsections.

363 *3.1. Pedestrian zone sizing*

364 Assuming policy makers wish to select a pedestrian zone size that does not cause trip demand to
 365 exceed roadway capacity, two constraints must be considered. First, the zone must be large enough
 366 to prevent traffic flow across the network from exceeding capacity $q_a(\gamma) < q_c$. Second, it must also
 367 be small enough to prevent perimeter traffic flow from also exceeding capacity $q_p(\gamma) < q_c$. Thus, a
 368 feasible pedestrian zone size can exist anywhere between $q_a(\gamma) \leq q_c \geq q_p(\gamma)$, as shown Figure 7.

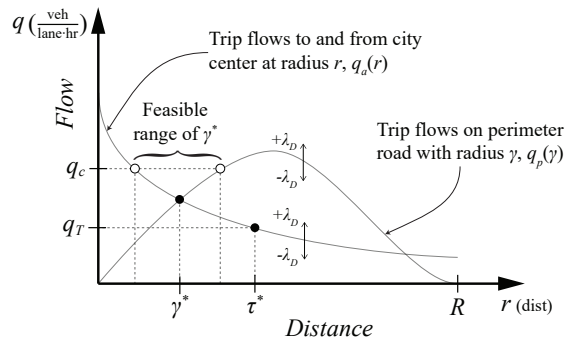


Figure 7: Pedestrian and transit priority zone size

369 However, this three point intersection of q_a , q_p , and q_c (as shown in Figure 7) is not guaranteed
 370 since the functions are independently affected by the two demand types (i.e., monocentric and
 371 baseline demand). The first constraint depends on the monocentric demand λ_c generating flow to
 372 and from the center, q_a . The second constraint depends on baseline demand λ_b generating flow
 373 around the perimeter road, q_p . This means that if one trip demand type is so low q_a or q_p never
 374 exceeds q_c in the positive space (i.e., when q and $r \geq 0$), then that constraint does not exist. This
 375 creates three possible cases:

- 376 (a) If both functions intersect with capacity, then $q_a(\gamma^*) \leq q_c \geq q_p(\gamma^*)$
- 377 (b) If $\lambda_c \ll \lambda_b$ so only q_a intersects with capacity, then $q_a(\gamma^*) \geq q_c$
- 378 (c) If $\lambda_c \gg \lambda_b$ so only q_p intersects with capacity, then $q_p(\gamma^*) \geq q_c$

379 While any point in these ranges are feasible, for mathematical convenience, the intersection points
 380 can be used to calculate pedestrian zone size. In case (b) and (c), this makes finding the solution
 381 relatively simple by setting the respective functions equal to roadway capacity q_c . This ensures

382 that the size is at least exactly small or large enough to meet capacity by selecting the minimum or
 383 maximum pedestrian zone size. However, in case (a) where both functions meet capacity, either point
 384 could be used. As a “compromise”, the intersection of the two flow functions could be used, ensuring
 385 both constraints are satisfied while the least possible traffic flow condition in either function is used.
 386 However, setting $q_a = q_p$ to find the intersection point results in a quintic function (polynomial to
 387 the 5th power):

$$f(\gamma) = \lambda_b \left(\frac{1}{R^2} \gamma^5 - \frac{1}{R} \gamma^4 - \gamma^3 \right) + \left(\lambda_b R + \frac{\lambda_c}{4\delta} \right) \gamma^2 - \frac{14R\lambda_b}{15\delta} \gamma - \frac{\lambda_c R^2}{4\delta} \quad (16)$$

388 yielding multiple points where the function is equal to zero (see Figure 8) and cannot be easily solved
 389 analytically.

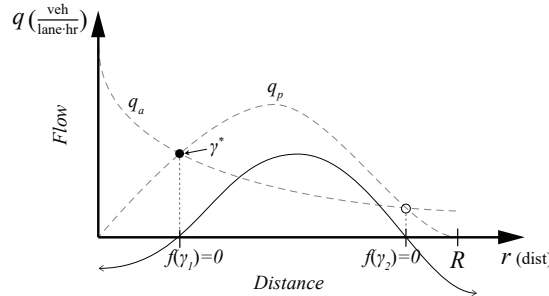


Figure 8: Quintic function for optimal compromise pedestrian zone size, $f(\gamma)$

390 Given that the pedestrian zone size must exist between $0 \leq \gamma \leq R$, the number of feasible solu-
 391 tions in the domain is reduced, allowing for an pedestrian zone dimension γ^* to be found numerically.
 392 Since two intersection points between q_a and q_p exist, the minimum of the two provides the desired
 393 optimal compromise, γ^* :

$$\begin{aligned} \gamma^* &\Leftarrow \min [f(\gamma_1) = 0, f(\gamma_2) = 0] \\ \text{s.t. } 0 &\leq \gamma \leq R \end{aligned} \quad (17)$$

394 To summarize, the pedestrianized zone essentially functions by “chopping off” traffic flow be-
 395 fore it exceeds capacity. The relative size of this zone is largely dependent on demand, increasing
 396 as monocentric demand increases, and decreasing as baseline demand increases. However, as the
 397 pedestrian zone size increases, average travel time also increase due to increasing walking distance
 398 and whatever unmitigated traffic remains outside of the zone. This section has addressed finding
 399 an appropriate pedestrian zone size, but has not yet considered traffic induced delay. Transit pri-
 400 ority can then be enacted to reduce travel time and offset some of this unmitigated traffic demand,
 401 essentially providing a stable travel time alternative to driving.

402 3.2. Transit priority zone size

403 The necessary transit priority zone size can be determined using the critical transit priority
 404 traffic flow q_T (see Figure 6). This value can be used in combination with network flow at distance
 405 r in Equation (1) to determine the necessary transit priority zone size, τ^* , when $q_T = q_a$. The
 406 reason that q_a is used, and not q_p , is because transit priority is concerned with traffic congestion
 407 experienced in the network outside of the pedestrian zone, not just at the perimeter. Solving then
 408 for $q_T = q_a$ yields a quadratic function, but assuming a non-negative value for the optimal transit
 409 zone size, it can be solved for analytically:

$$\tau^*(\Phi_D) = \frac{56\Phi_D\lambda_b - 60\delta q_T + \sqrt{(56\Phi_D\lambda_b - 60\delta q_T)^2 + (30\Phi_D\lambda_c R)^2}}{30\Phi_D\lambda_c} \quad (18)$$

s.t. $\tau^* \geq 0$

410 where the proportion of driving trips, Φ_D , is introduced to scale driving demand to account for
 411 mode choice between driving and transit. Unlike the optimal pedestrian zone, which is unaffected
 412 by changes in driving demand, the optimal transit priority zone size will depend on driving demand.
 413 This is because, assuming λ_c and λ_b are affected by mode choice equally, both q_a and q_p shift
 414 vertically, keeping γ^* constant (See Figure 7).

415 Although the proportion Φ_D may be modeled as a discrete choice probability, this requires travel
 416 time as an input, making optimal τ difficult to find as it creates a dynamic problem. Fortunately,
 417 since since γ^* remains constant relative to demand, the necessary proportion of driving demand Φ_D
 418 to achieve $q_a = q_T$ (see Figure 8) can be determined directly as a function of τ :

$$\Phi_D(\tau) = \frac{-60\delta\tau q_T}{15\tau^2\lambda_c - 56\tau\lambda_b - 15\lambda_c R^2} \quad (19)$$

419 With the proportion of drivers, Φ_D , determined as a function of transit priority zone size, τ ; the
 420 travel time function in Equation (14) is now dependent on only the pedestrian and transit priority
 421 zone sizes of γ and τ , respectively.

422 3.2.1. Relationship of demand and transit priority zone size

423 It should be very clearly stated here that this Φ_D is *not* mode choice per se, but merely the
 424 proportion of driving demand so that driving travel time is equal to transit priority travel time for
 425 the given τ . The inferred assumption here is that mode choice depends solely on travel time and
 426 is equally substitutable, meaning that travelers do not have a preference for driving over transit.
 427 This, of course, is a gross over assumption, but for simplicity this analysis will carry on with this
 428 assumption. However, future models might calibrate by assuming some proportionally weighted
 429 travel time cost to account for mode preference. For example, transit travel costs w more than
 430 driving, e.g., $t_{transit} = wt_{drive}$. This would have the effect of increasing q_T and τ , meaning that
 431 travelers are willing to tolerate more time in traffic before they step foot on a bus.

432 An interesting caveat to this function is that unlike true mode choice, the function for the
 433 proportion of driving demand, Φ_D , can go beyond 0 and 1. If it exceeds 1 this means that more
 434 than 100% of demand must drive in order to achieve $q_a = q_T$ for a transit priority zone size of τ .
 435 This occurs when traffic conditions do not reach the level necessary to justify transit priority at
 436 τ , and a smaller τ must be chosen to increase driving demand. This may seem like an erroneous
 437 outcome of the model, but is actually a useful way to determine if a transit priority zone of size τ is
 438 appropriate. If the transit priority zone size is already the smallest it can be (i.e., $\tau = \gamma$ or $\tau = 0$),
 439 then this means that transit priority is never justifiable because there is not enough overall travel
 440 demand in the city itself for $q_a = q_T$. Conversely, the function can also yield a negative value if
 441 $\tau < 0$. However, this would require a negative demand or negative transit priority zone.

442 This Φ_D function can be used to explore transit priority applicability. When total demand in the
 443 city varies, it alters the steepness of the driving proportion function, Φ_D , as τ varies (see Figure 9a).
 444 For a fixed transit priority zone of size τ , and varying overall travel demand λ , the zone is justified
 445 when $\Phi_D \leq 1$ (see Figure 9b). Meaning automobile traffic conditions are at least the same travel
 446 time or slower than transit priority. For example, if the traffic flow at the edge of the pedestrian
 447 zone is less than the transit priority threshold, $q_a(\gamma) < q_T \Rightarrow \Phi_D > 1$, a driving demand greater
 448 than the total travel demand is needed and a transit priority zone is not beneficial.

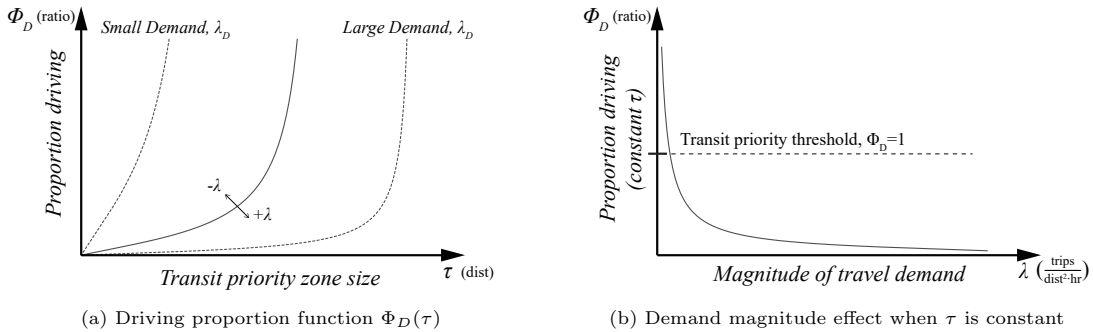


Figure 9: Demand magnitude effect on proportion

449 4. Numeric application

450 To demonstrate the hypothetical outcomes of a pedestrianized zone surrounded by a transit
 451 priority zone, numeric input parameters provided in Table 1 for calculation. These parameters are
 452 loosely derived from a real-world case in Melbourne, Australia, shown in Figure 10.

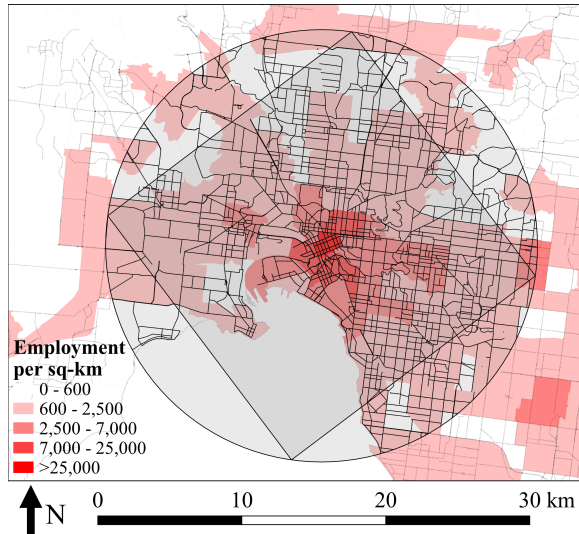


Figure 10: Street Network and Employment Density in Melbourne, Australia

453 Melbourne provides a useful example to draw from because it is a highly monocentric and au-
 454 tomobile dependent city with a sprawling and relatively uniform rectilinear street network with
 455 few geographic interruptions other than the bay. This enables parameters to be determined fairly
 456 easily using Geospatial Information Systems (GIS) and census sources. Moreover, Melbourne also
 457 currently has a partially pedestrianized Central Business District (CBD) and a large mixed-traffic
 458 streetcar system (called trams in Australia) which suffers from congestion, making it an intriguing
 459 case to draw from.

Table 1: Input Parameters

| Parameter | Value | Units |
|-------------|--------------------|---------------------------------|
| R | 15 | km |
| δ | 2.8 | lane · dist / dist ² |
| λ_b | 67 | trips / km ² · hr |
| λ_c | 60 | trips / km ² · hr |
| v_m | 50 | km/hr |
| v_w | 5 | km/hr |
| t_s | 60 | sec |
| s | 0.5 | km |
| k_c | 45 | veh/k |
| q_c | 500 | trips / lane · hr |
| d | $2/\delta = 0.714$ | km |

460 4.1. Baseline scenario – no pedestrian or transit priority policies

461 First, a baseline scenario in a city with no pedestrianized or transit priority zones using the
462 numeric parameters from Table 1, demand is varied in Figure 11 by shifting the proportion of total
463 demand that drives or uses transit. Again, for demonstration purposes, this assumes infinite transit
464 capacity. The travel time of both mixed-traffic transit and driving dramatically increase as driving
465 demand increases. This is because the network reaches capacity and traffic flow breaks down, it
466 causes average travel time for both driving and mixed-traffic transit to dramatically increase.

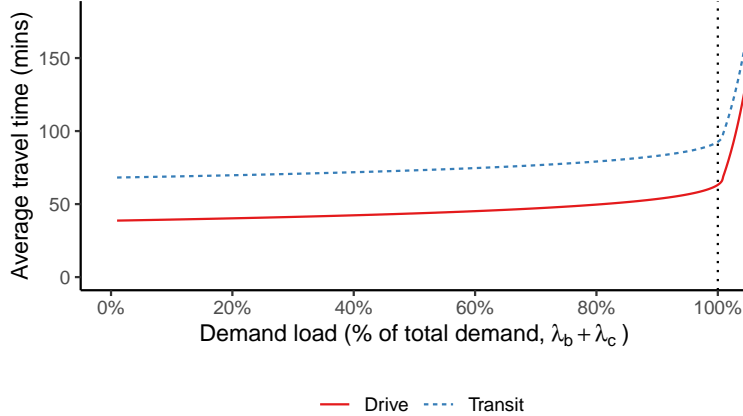


Figure 11: Average total travel time varying demand with no pedestrian zone or transit priority

467 It is also clear that transit demand is always slower than driving demand, even if the difference
468 between the two modes becomes arbitrarily small as the average travel time becomes dramatically
469 large. This numerically illustrates the situation hypothesized in Figure 6. As mentioned, the problem
470 in this scheme is there is little or no incentive for an individual to choose transit, other than out of
471 necessity or to altruistically improve the system for all.

472 4.2. Independent pedestrian and transit priority policies

473 While it is unrealistic that travel time would approach infinity, one might assume that as traf-
474 fic flow breaks down and travel time dramatically increases, demand for travel itself might simply
475 become suppressed in general. To avoid such a scenario, ensuring that travel demand is not sup-
476 pressed and able to travel freely, the city might decide to impose a pedestrianized or transit priority

477 zone. Figure 12 demonstrates the effect of pedestrianized and transit priority zones on the respective
 478 average travel time of driving and transit.

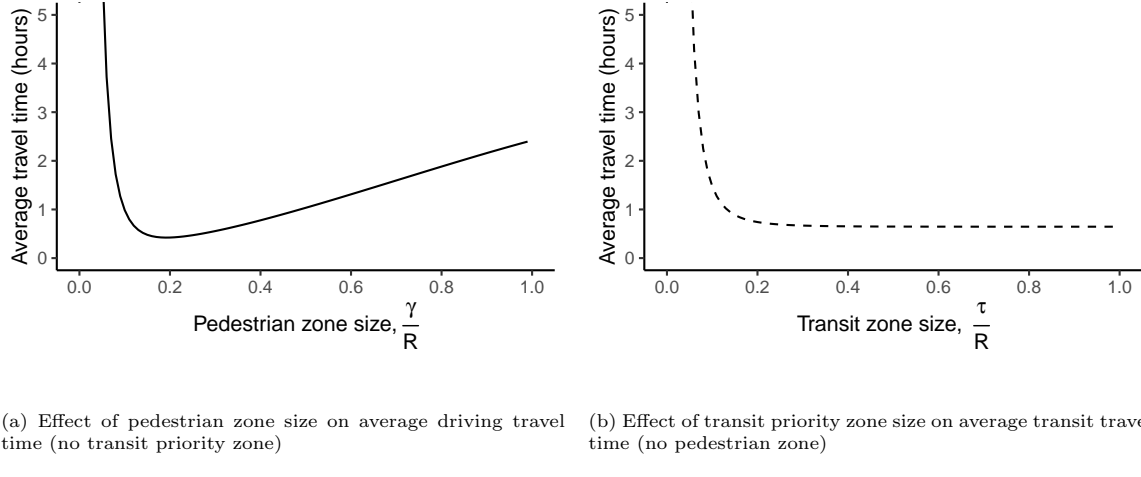


Figure 12: Average travel time by mode varying pedestrian and transit zone size, γ and τ

479 Both Figures 12a and 12b decrease in travel time as the zone sizes increase. This is because
 480 the most extreme congestion in the very center of the city is effectively abolished, thus yielding a
 481 huge improvement but with diminishing returns. However, in the driving case the travel time begins
 482 to increase as the pedestrianized zone become unreasonably large, effectively trading driving for
 483 walking.

484 A caveat in this model is that both Figures 12a and 12b approach infinity as the zone size
 485 becomes infinitesimally small. From a mathematical perspective, this is an artifact of the piece-wise
 486 monotonic function approaching infinity as the travel demand exceeds available roadway capacity on
 487 the perimeter road (i.e., when $q \geq q_c : t(q) = t_c (q/q_c)^{20}$). More intuitively, this extreme boundary
 488 condition occurs when the pedestrian or transit priority zone becomes so small that there simply is
 489 not enough road infrastructure to carry the vehicles around the city center.

490 The reason why Figure 12 is unaffected by this condition is that when the pedestrian and transit
 491 priority zones are a size of exactly zero, they do not exist at all and do not create this condition. In
 492 reality, this is somewhat confounding that traffic congestion would suddenly jump to infinity as a
 493 transit or pedestrian zone size increases from zero to some tiny zone size, $d/d\tau$. However, one realistic
 494 constraint is that a pedestrian or transit priority zone size cannot feasibly be smaller than one city
 495 block, or else there would be no road infrastructure to carry the vehicles. Assuming a street spacing
 496 of s , this can be used to arbitrarily define a boundary for the minimum feasible zone size, $\gamma \geq s$ and
 497 $\tau \geq s$, for pedestrian and transit priority zones, respectively.

498 4.3. Transit priority threshold

499 To determine whether traffic conditions are worse enough to justify transit priority, regardless
 500 of a pedestrianized zone, the driving demand proportion, Φ_D , can be evaluated against the transit
 501 priority threshold, $\Phi_D = 1$. To demonstrate the transit priority threshold, Figure 13 shows a range
 502 of transit priority zone sizes across a varying demand load.

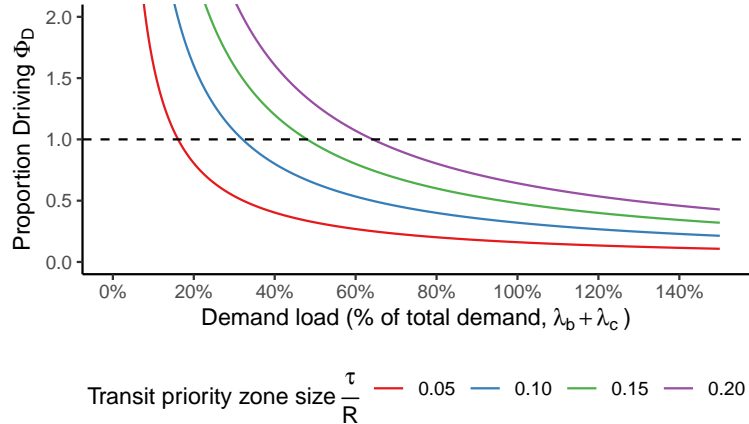


Figure 13: Demand loading to justify transit priority

503 Figure 13 shows that as demand load increases, the threshold decreases (as also shown in Figure
 504 9b). Conversely, as the transit priority zone becomes larger (e.g., $\frac{\tau}{R}$ from 0.05 to 0.20), the
 505 threshold effectively increases. This is because traffic congestion decreases further from the center.
 506 However, this also means that just because a large transit priority zone of a certain size does not
 507 meet the threshold, it does not mean transit priority is entirely inappropriate, only that a smaller
 508 zone may be required.

509 4.4. Combined pedestrian and transit priority policies

510 Figures 12a and 12b only consider travel time independently of the modes, and does not consider
 511 the combined effect on the average travel time of both modes. Meaning, they do not account for the
 512 effect that a pedestrian zone might have on travel time with a transit zone and vice versa. Figure 14
 513 shows the combined average travel for both modes as the pedestrianized and transit priority zone
 514 vary in size. For demonstration, the transit priority zone is shown as being some proportion of the
 515 pedestrianized zone, ranging from being the same size as the pedestrianized zone (i.e., no transit priority
 516 zone) to four times the size of the pedestrianized zone.

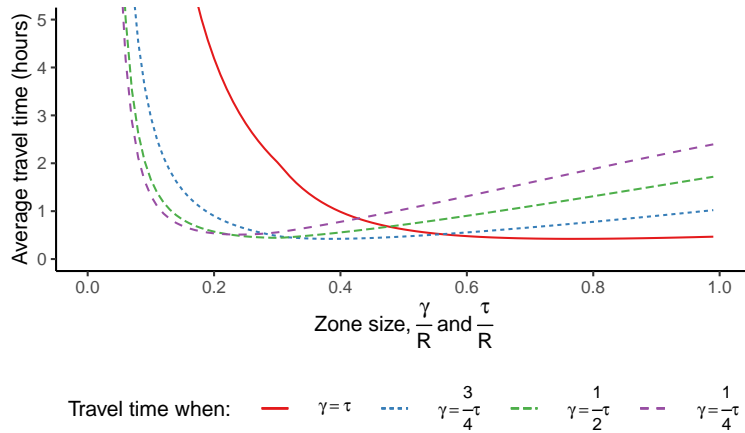


Figure 14: Average combined travel time for transit and driving varying τ and γ

517 4.5. Optimal pedestrian and transit priority zone sizes

518 It is clear from Figure 14 that the optimal travel time can vary with both the pedestrianized
 519 and transit priority zone sizes. To visualize this bi-variate gradient, the travel time in Figure 15
 520 is plotted against both the pedestrian zone on the horizontal axis, and the transit priority zone on
 521 the vertical axis. The shaded diagonal half of the plot represents when the transit priority zone is
 522 less than the pedestrian zone size. While a result can be calculated, it makes little sense in reality
 523 to have such a condition. Thus, any point below the diagonal can be considered outside of feasible
 524 space, simplifying optimization.

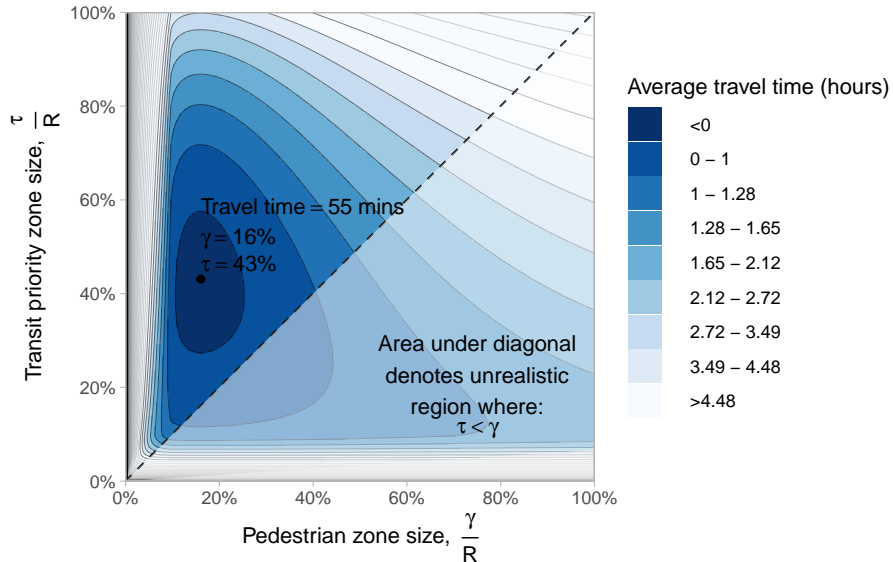


Figure 15: Average total travel time varying across γ and τ

525 In this case, the optimal pedestrianized and transit priority zone sizes are 16% and 43% of R ,
 526 respectively; with a minimum average travel time of 0.92 hours. It is interesting that the transit
 527 priority zone is only 170% larger (27% of R) than the pedestrianized zone. This suggests that the
 528 majority of the travel time improvement is achieved through pedestrianization, and that the transit
 529 priority zone mainly serves to mitigate the perimeter road congestion. The optimal travel time
 530 gradient surface in Figure 15 is also fairly stable, allowing room for error. Slightly over sized zones
 531 would not result in any appreciable loss in performance.

532 4.6. Network capacity of combined pedestrian and transit priority policies

533 Recalling the breakdown of traffic flow in Figure 11, the optimal policy for a varying demand
 534 loading is shown in comparison in Figure 16. The optimal case not only provides a lower average
 535 travel time initially, but also does not break down as severely. After a certain level of demand the
 536 optimal travel time appears to plateau, this is because the entire city has been zoned as transit
 537 priority, establishing a stable travel average time. If the total city extents were larger (i.e., a larger
 538 R), the optimal case might continue its gradual increase. However, a larger city extent would mean
 539 the traffic density in the city center is proportionally increased, thus worsening the breakdown point.

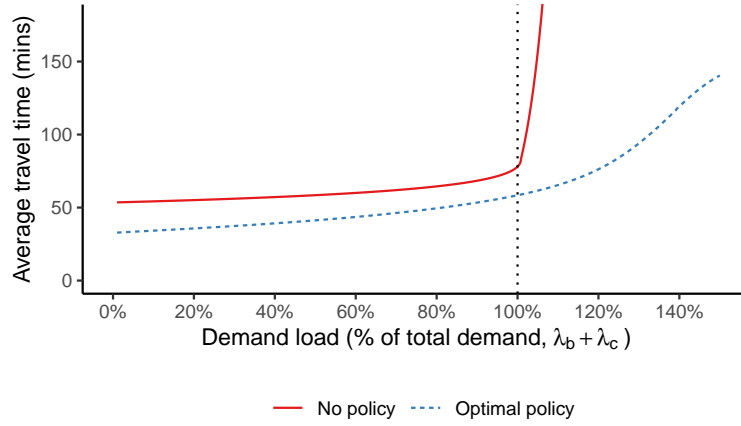
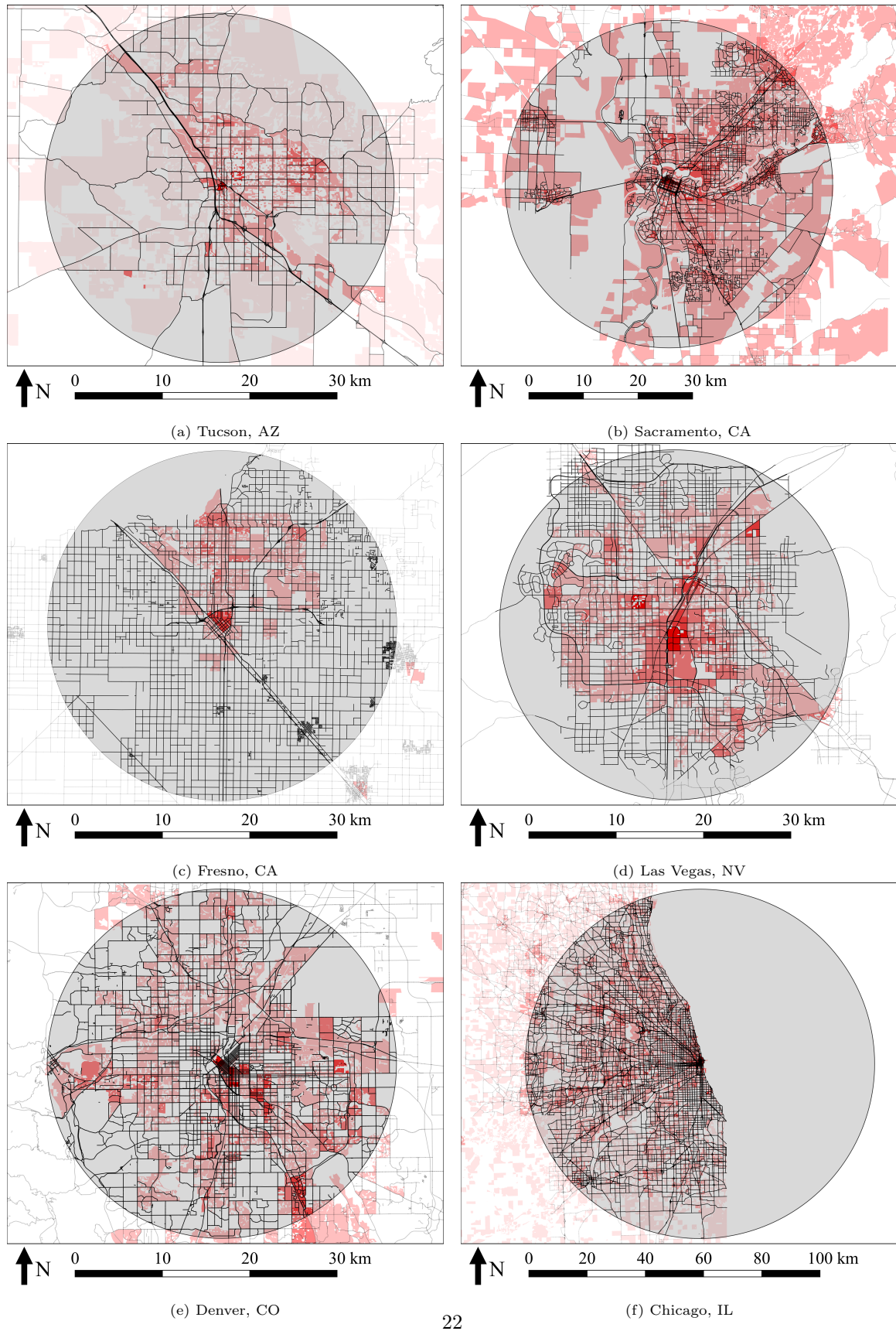


Figure 16: Comparing average total travel time for no policy and optimal pedestrian and transit priority policies

540 *4.7. Supplemental comparative analysis*

541 To further explore the relative application of the proposed model beyond Melbourne, Australia;
 542 six additional cities are analyzed. These six cities are Tucson, Arizona; Sacramento, California;
 543 Fresno, California; Las Vegas, Nevada; Denver, Colorado; and Chicago, Illinois. As shown in Fig-
 544 ure 17), all of the cities possess a robust rectilinear street network and some level of monocentricity
 545 in the form of centrally concentrated employment density. It is important to note that these densities
 546 are employment densities, not housing density. Employment density was chosen to better reflect the
 547 relative distribution of trip destinations, regardless of origin.



548 A summary of results and additional density distribution statistics are presented in Table 2. The
 549 city street networks vary due to geography and land use (e.g., proximity to agriculture, mountains,
 550 and bodies of water), but still largely maintain a fairly uniformly grid-like street network where
 551 possible. However, an interesting difference is the variation in overall employment density and the
 552 distribution of density in each city. Figure 18 demonstrates the relative variation in employment
 553 density across the different cities. Chicago is the largest, densest city, and likely the most monocen-
 554 tric city of the group with the highest average density and standard deviation of density of 3,869 and
 555 13,696 jobs per square kilometer, respectively. This is evident in Figure 18a, with Chicago main-
 556 taining a relatively high density beyond where most cities begin to taper off. Fresno and Tucson
 557 possess the lowest density, which is likely proportional to their overall population, but Tucson does
 558 have a much higher standard deviation relative to its mean density, indicating there may be pockets
 559 of very high density.

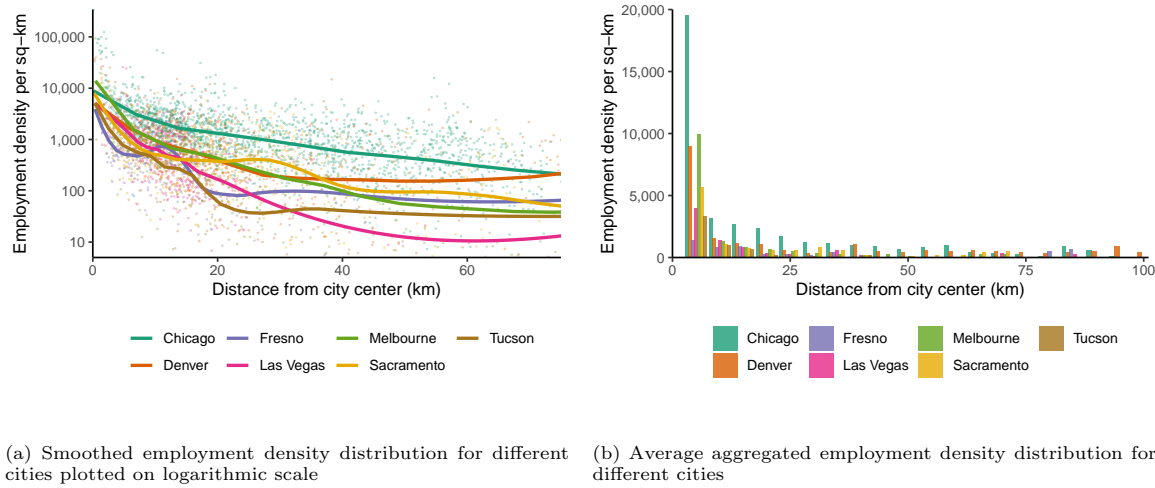


Figure 18: Distribution of employment density by distance from city center for different cities

560 The trip demand parameters, λ_c and λ_b , are roughly approximated from the statistical values
 561 of employment density for each city. Baseline trip demand, λ_b , is calculated as median employment
 562 density divided by the number of daytime travel hours (15 hours from 5am to 8pm). Monocentric
 563 demand, λ_c , is calculated as the mean density divided by the coefficient of variation (i.e., ratio of
 564 mean to standard deviation) divided by number of daytime travel hours. This procedure is highly
 565 generalized and does not capture the true spatial monocentricity of trip density. Furthermore, the
 566 street network density is also roughly approximated using only the *major* streets defined by local
 567 jurisdictions (e.g., arterial functional classification). This not only ignores local streets that may
 568 carry network traffic, but also does not capture any potential asymmetric network densities (e.g.,
 569 road network is densest in the center and less dense at the edges). However, the procedure described
 570 is sufficient for systematically extracting basic demand parameters for demonstrating the proposed
 571 model.

Table 2: Multi-city analysis results and statistics

| City | Employment density statistics | | | | | | | Avg. | | | |
|------------|-------------------------------|--------|----------|-----------|-----|----------|-------------|-------------|----------|--------|-------------|
| | Mean | Median | Std Dev. | n zones | R | δ | λ_c | λ_b | γ | τ | travel time |
| Chicago | 3,869 | 1,824 | 13,696 | 1,075 | 30 | 2.4 | 73 | 122 | 8.7 | 14.5 | 117 |
| Denver | 1,613 | 757 | 3,609 | 356 | 20 | 2.7 | 48 | 50 | 4.0 | 6.6 | 83 |
| Fresno | 931 | 514 | 1,325 | 154 | 20 | 2.0 | 44 | 34 | 4.2 | 7.7 | 81 |
| Las Vegas | 1,249 | 735 | 2,396 | 428 | 20 | 2.6 | 43 | 49 | 3.8 | 7.1 | 82 |
| Melbourne | 2,886 | 1,000 | 9,192 | 112 | 15 | 2.8 | 60 | 67 | 2.4 | 4.9 | 58 |
| Sacramento | 1,310 | 499 | 3,239 | 356 | 30 | 2.8 | 35 | 33 | 5.7 | 11.6 | 121 |
| Tucson | 1,086 | 424 | 2,877 | 186 | 20 | 1.8 | 27 | 28 | 2.3 | 7.7 | 71 |

572 The results shown in Table 2 yields a pedestrianized zone surrounded by a transit priority zone
 573 in each city, but varying in sizes. Unsurprisingly Chicago yields the largest zones of radius 8.7 km
 574 and 14.5 km, respectively. Pedestrianization would encompass most of the inner neighborhoods,
 575 approximately halfway to Chicago Midway Airport, and transit priority to just beyond Midway
 576 Airport. While full pedestrianization at this scale is impractical, partial pedestrianization that
 577 discourages through traffic is more realistic. Transit priority is less unrealistic, with transit in this
 578 zone already being well serviced by Chicago’s urban rail system. In contrast, Sacramento yielded
 579 a surprisingly large transit priority zone considering the city’s low density sprawl. This may be a
 580 result of the large proportion of monocentric demand to baseline demand.

581 It should be strongly stated that these results very rough. However, the results do provide
 582 interesting general insight and also demonstrate the applicability of this model. It is possible that
 583 future applications could implement the model on a more localized neighborhood-scale to better suit
 584 polycentric cities.

585 5. Discussion

586 While the model can be utilized for the immediate purpose of determining optimal zone sizing,
 587 traffic flow characteristics, and travel time across the city’s street network; this is not necessarily
 588 practical as the model is based on an idealized city, nor is the primary purpose in this paper. The
 589 key objective is to demonstrate the complementary benefits of pedestrianized and transit priority
 590 zones in a city. However, the model presented is highly idealized. In reality most cities are incredibly
 591 complex, diverse, and asymmetric. Furthermore, the model also does not account for the multitude
 592 of social and behavioral factors that often play a critical role in transportation and urban systems.
 593 To summarize, the model possesses four critical weaknesses:

594 The model does not account for suppressed demand. Comparing the base case with the optimal
 595 case, it is clear that the pedestrianization and transit priority zones enable 100% of demand to be
 596 served without the severe breakdown in traffic flow observed in the base case in Figure 11. In reality
 597 the network would likely not reach such extreme traffic flow break down as demand would simply
 598 be suppressed, with a certain portion of demand choosing to use transit out of necessity (e.g., low
 599 income), convenience (e.g., commuter rail), or various other factors; ultimately finding some other
 600 equilibrium point. However, this is not necessarily a model flaw, but is important as this suppressed
 601 equilibrium point is sub-optimal, resulting in depressed mobility, dampened economic activity, and
 602 lacks the social and environmental benefits of a dense pedestrian oriented city center. This is a
 603 critical issue, merely managing demand through harsh travel restrictions or economic policies (e.g.,
 604 road-space rationing or tolls) with no reasonable alternative serves only to suppress demand and
 605 activity. Moreover, this can also have severe equity implications by disproportionately restricting
 606 access to jobs and leisure, burdening those who cannot easily afford higher-cost road pricing or
 607 circumvent travel restrictions. This point is particularly important, considering pedestrianization is
 608 generally intended to provide a social benefit.

609 The model has no account for cost or pricing. This is a critical weakness, not only in terms of
610 mode-choice modeling, but in accounting for “softer” economic policies, such as congestion pricing
611 (e.g., London, Stockholm, and New York City), that are less aggressive than physical barriers and
612 alleviate the freight and emergency services issue. This is conceptually similar in that it reduces
613 automobile usage in a zone (albeit through economic barriers), but is important practically as
614 it allows for a transfer of funds from one mode to another. This is especially important when
615 considering equity impacts of exclusionary policies. However, monetary costs could be incorporated
616 into future models by converting to temporal costs. Such a model would further benefit from a
617 heterogeneous population of travelers in order to measure equity impacts.

618 The model assumes infinite transit capacity with no congestion impacts. Although transit has
619 the potential to offer substantially higher capacity than single occupancy automobiles, limits do
620 exist and transit service is often impacted by passenger congestion (e.g., increased dwell time from
621 door crowding). For clarity it was assumed that transit priority offers reliable service relative to
622 automobiles, but these considerations could be accounted for in future models. Furthermore, this
623 model is highly generalized and assumes no impact on automobile congestion from transit priority.
624 While this may be true for vertically separated transit right-of-ways, such as elevated tracks or
625 subways, this may not be true for at-grade space allocation, such as dedicated bus lanes.

626 The model assumes uniform pedestrianization and transit priority zoning. In reality it is possible
627 that certain streets or partial pedestrianization can happen. This also ignores practical issues such
628 as emergency services and freight delivery. For example, San Francisco’s Market Street prohibits
629 private automobiles, but allows delivery vehicles and taxis. There also exists a spectrum of transit
630 priority, from transit signal priority only, to a fully separated right-of-way. Future research could
631 address this using some priority/pedestrianization scale (e.g., from 0 to 100%) to account for this
632 effect, rather than a binary transit priority and pedestrianized zone.

633 Despite these weaknesses, the model does offer valuable insights on pedestrianization and transit
634 priority policies. The major finding from this analysis is the travel time benefit and network capacity
635 gained with the optimal pedestrian and transit priority zone compared to the base case with no
636 policy intervention (see Figure 16). In addition, the model also provides a potentially useful tool in
637 determining the overall travel demand threshold where transit priority is justifiable.

638 6. Conclusion

639 As countless urban planners have sought to articulate, dense walkable city centers offer a plethora
640 of benefits. From more efficient land-use utilization with less land dedicated to roads, highways and
641 parking; environmental gains from reduced emissions and the urbanized footprint; public health
642 gains from active transportation (e.g., walking and biking) and improved air quality; to economic
643 growth and resiliency by reducing congestion and unlocking potentially suppressed travel demand.
644 The analytical model developed in this paper seeks to validate this by objectively demonstrating the
645 potential complementary benefits to travel time with a pedestrianized zone surrounded by a transit
646 priority zone in a city with a rectilinear street network.

647 The optimal case with pedestrianized and transit priority zones not only provided a pedestrian
648 oriented city center, meeting social objectives, but also greatly increased the network capacity of
649 the city, satisfying the engineering and economic objectives. Overall, the analytical model reveals
650 general insight on the complementary benefits of pedestrianized and transit priority zones in allowing
651 greater network capacity while providing desirable pedestrian oriented urbanism. Insights from this
652 analysis are most directly applicable to large dense cities with robust existing transit systems, but
653 could also be used with smaller cities to approximate when pedestrianization and transit priority
654 is, or is not, effective. Furthermore, while the model lacks several important considerations (e.g.,
655 transit capacity, non-binary zoning, pricing, and heterogeneous travelers), it firmly establishes the
656 fundamentals that could be easily expanded in future work.

657 **Acknowledgments**

658 The author would like to acknowledge Dr. Gonzales of the University of Massachusetts Amherst
659 for the initial formulation of network traffic flow in a circular city [60, 65, 74], from which this model
660 was originally conceived.

661 **References**

- 662 [1] R. M. Solow, W. S. Vickrey, Land use in a long narrow city, *Journal of Economic Theory* 3 (4)
663 (1971) 430–447. doi:10.1016/0022-0531(71)90040-8.
- 664 [2] R. M. Solow, Congestion, Density and the Use of Land in Transportation, *The Swedish Journal
665 of Economics* 74 (1) (1972) 161. doi:10.2307/3439015.
- 666 [3] R. M. Solow, Congestion Cost and the Use of Land for Streets, *The Bell Journal of Economics
667 and Management Science* 4 (2) (1973) 602. doi:10.2307/3003055.
- 668 [4] A. Anas, R. Arnott, K. A. Small, Urban Spatial Structure, *Journal of Economic Literature*
669 36 (3) (1998) 1426–1464. arXiv:arXiv:1011.1669v3, doi:10.2307/2564805.
- 670 [5] A. Anas, R. Xu, Congestion, Land Use, and Job Dispersion: A General Equilibrium Model,
671 *Journal of Urban Economics* 45 (3) (1999) 451–473. doi:10.1006/juec.1998.2104.
- 672 [6] W. C. Wheaton, Land Use and Density in Cities with Congestion, *Journal of Urban Economics*
673 43 (2) (1998) 258–272. doi:10.1006/juec.1997.2043.
- 674 [7] E. Rossi-Hansberg, Optimal urban land use and zoning, *Review of Economic Dynamics* 7 (1)
675 (2004) 69–106. doi:10.1016/S1094-2025(03)00056-5.
- 676 [8] S. Yagar, B. Han, A procedure for real-time signal control that considers transit interfer-
677 ence and priority, *Transportation Research Part B* 28 (4) (1994) 315–331. doi:10.1016/0191-
678 2615(94)90004-3.
- 679 [9] S. Yagar, Efficient Transit Priority at Intersections, *Transportation Research Record* 1390 (1993)
680 77.
- 681 [10] A. Nash, Implementing Zurich’s Transit Priority Program, *Transportation Research Record:
682 Journal of the Transportation Research Board* 1835 (1) (2003) 59–65. doi:10.3141/1835-08.
- 683 [11] J. G. Wardrop, Some Theoretical Aspects of Road Traffic Research, *Proceedings of the institu-
684 tion of civil engineers* 1 (3) (1952) 325–362.
- 685 [12] E. J. Gonzales, C. F. Daganzo, The evening commute with cars and transit: duality results and
686 user equilibrium for the combined morning and evening peaks, *Transportation Research Part
687 B: Methodological* 57 (2013) 286–299.
- 688 [13] T. Tabuchi, Bottleneck Congestion and Modal Split, *Journal of Urban Economics* 34 (3) (1993)
689 414–431. doi:10.1006/juec.1993.1044.
- 690 [14] W. S. Vickrey, Congestion Theory and Transport Investment, *The American Economic Review*
691 59 (2) (1969) 251–260.
- 692 [15] Z.-C. Li, Y.-D. Wang, W. H. K. Lam, A. Sumalee, K. Choi, Design of Sustainable Cordon Toll
693 Pricing Schemes in a Monocentric City, *Networks and Spatial Economics* 14 (2) (2014) 133–158.
694 doi:10.1007/s11067-013-9209-3.

- 695 [16] Y. Lou, Y. Yin, S. Lawphongpanich, Robust congestion pricing under boundedly rational user
696 equilibrium, *Transportation Research Part B: Methodological* 44 (1) (2010) 15–28.
- 697 [17] H.-J. Huang, Pricing and logit-based mode choice models of a transit and highway system
698 with elastic demand, *European Journal of Operational Research* 140 (3) (2002) 562–570.
699 doi:10.1016/S0377-2217(01)00228-4.
- 700 [18] J. Y. Wang, H. Yang, R. Lindsey, Locating and pricing park-and-ride facilities in a linear mono-
701 centric city with deterministic mode choice, *Transportation Research Part B: Methodological*
702 38 (8) (2004) 709–731. doi:10.1016/j.trb.2003.10.002.
- 703 [19] H. Yang, M. G. H. Bell, Traffic restraint, road pricing and network equilibrium, *Transportation
704 Research Part B: Methodological* 31 (4) (1997) 303–314.
- 705 [20] N. Zheng, R. A. Waraich, K. W. Axhausen, N. Geroliminis, A dynamic cordon pric-
706 ing scheme combining the Macroscopic Fundamental Diagram and an agent-based traf-
707 fic model, *Transportation Research Part A: Policy and Practice* 46 (8) (2012) 1291–1303.
708 doi:10.1016/j.tra.2012.05.006.
- 709 [21] H.-J. Huang, Fares and tolls in a competitive system with transit and highway: the case with two
710 groups of commuters, *Transportation Research Part E: Logistics and Transportation Review*
711 36 (4) (2000) 267–284.
- 712 [22] E. J. Gonzales, C. F. Daganzo, Morning commute with competing modes and distributed
713 demand: user equilibrium, system optimum, and pricing, *Transportation Research Part B:
714 Methodological* 46 (10) (2012) 1519–1534.
- 715 [23] R. Danielis, E. Marcucci, Bottleneck road congestion pricing with a competing railroad service,
716 *Transportation Research Part E: Logistics and Transportation Review* 38 (5) (2002) 379–388.
- 717 [24] R. Brambilla, G. Longo, B. Rudofsky, *For Pedestrians Only: Planning, Design, and Manage-
718 ment of Traffic-free Zones*, Whitney library of design, Whitney Library of Design, 1977.
- 719 [25] B. Pushkarev, *Urban space for pedestrians*, MIT press (1975).
- 720 [26] D. Engwicht, *Reclaiming Our Cities and Towns: Better Living with Less Traffic*, New Catalyst,
721 1993.
- 722 [27] W. Owen, *The Accessible City*, Brookings Institution (1973).
- 723 [28] E. W. Walbridge, A transit-oriented city, *Transportation Research Record* (658) (1977).
- 724 [29] A. Skabardonis, Control Strategies for Transit Priority, *Transportation Research Record: Jour-
725 nal of the Transportation Research Board* 1727 (1) (2000) 20–26. doi:10.3141/1727-03.
- 726 [30] F. Dion, B. Hellinga, A rule-based real-time traffic responsive signal control system with transit
727 priority: application to an isolated intersection, *Transportation Research Part B: Methodolog-
728 ical* 36 (4) (2002) 325–343. doi:10.1016/S0191-2615(01)00006-6.
- 729 [31] F. Dion, H. Rakha, Y. Zhang, Evaluation of Potential Transit Signal Priority Benefits along a
730 Fixed-Time Signalized Arterial, *Journal of Transportation Engineering* 130 (3) (2004) 294–303.
731 doi:10.1061/(ASCE)0733-947X(2004)130:3(294).
- 732 [32] J. Stevanovic, A. Stevanovic, P. T. Martin, T. Bauer, Stochastic optimization of traffic control
733 and transit priority settings in VISSIM, *Transportation Research Part C: Emerging Technologies*
734 16 (3) (2008) 332–349. doi:10.1016/j.trc.2008.01.002.

- 735 [33] M. Mesbah, M. Sarvi, I. Ouveysi, G. Currie, Optimization of transit priority in the transportation
736 network using a decomposition methodology, *Transportation Research Part C: Emerging Technologies* 19 (2) (2011) 363–373. doi:10.1016/j.trc.2010.05.020.
- 738 [34] W. Ma, W. Ni, L. Head, J. Zhao, Effective Coordinated Optimization Model for Transit Priority
739 Control under Arterial Progression, *Transportation Research Record: Journal of the Transportation
740 Research Board* 2366 (1) (2013) 71–83. doi:10.3141/2356-09.
- 741 [35] M. Mesbah, M. Sarvi, G. Currie, New Methodology for Optimizing Transit Priority at the
742 Network Level, *Transportation Research Record: Journal of the Transportation Research Board*
743 2089 (1) (2008) 93–100. doi:10.3141/2089-12.
- 744 [36] T. W. Sanchez, Poverty, policy, and public transportation, *Transportation Research Part A: Policy
745 and Practice* 42 (5) (2008) 833–841. doi:10.1016/j.tra.2008.01.011.
- 746 [37] Z. Wang, J. Wang, D. He, Transit Policies and Potential Carbon Dioxide Emission Impacts,
747 *Transportation Research Record: Journal of the Transportation Research Board* 2287 (1) (2012)
748 98–104. doi:10.3141/2287-12.
- 749 [38] G. F. Newell, Scheduling, Location, Transportation, and Continuum Mechanics: Some Simple
750 Approximations to Optimization Problems, *SIAM Journal on Applied Mathematics* 25 (3)
751 (1973) 346–360. doi:10.1137/0125037.
- 752 [39] H. Badia, J. Argote-Cabanero, C. F. Daganzo, How network structure can boost and shape the
753 demand for bus transit, *Transportation Research Part A: Policy and Practice* 103 (2017) 83–94.
- 754 [40] H. Badia, M. Estrada, F. Robusté, Competitive transit network design in cities with radial
755 street patterns, *Transportation Research Part B: Methodological* 59 (2014) 161–181.
756 doi:10.1016/j.trb.2013.11.006.
- 757 [41] H. Chen, W. Gu, M. J. Cassidy, C. F. Daganzo, Optimal transit service atop ring-radial and grid
758 street networks: A continuum approximation design method and comparisons, *Transportation
759 Research Part B: Methodological* 81 (2015) 755–774. doi:10.1016/j.trb.2015.06.012.
- 760 [42] C. F. Daganzo, Structure of competitive transit networks, *Transportation Research Part B:
761 Methodological* 44 (4) (2010) 434–446. doi:10.1016/j.trb.2009.11.001.
- 762 [43] E. M. Holroyd, The optimum bus service: a theoretical model for a large uniform urban area, in:
763 *Proceedings of the Third International Symposium on the Theory of Traffic Flow - Operations
764 Research Society of America*, 1967, pp. 308–328.
- 765 [44] K. Sivakumaran, Y. Li, M. J. Cassidy, S. Madanat, Cost-saving properties of schedule coordination
766 in a simple trunk-and-feeder transit system, *Transportation Research Part A: Policy
767 and Practice* 46 (1) (2012) 131–139. doi:10.1016/j.tra.2011.09.013.
- 768 [45] R. Vaughan, *Urban spatial traffic patterns.*, Pion Limited, 1987.
- 769 [46] R. B. Dial, Bicriterion traffic assignment: basic theory and elementary algorithms, *Transportation
770 science* 30 (2) (1996) 93–111.
- 771 [47] D. Watling, User equilibrium traffic network assignment with stochastic travel times and late
772 arrival penalty, *European journal of operational research* 175 (3) (2006) 1539–1556.
- 773 [48] A. Chen, J.-S. Oh, D. Park, W. Recker, Solving the bicriteria traffic equilibrium problem with
774 variable demand and nonlinear path costs, *Applied Mathematics and Computation* 217 (7)
775 (2010) 3020–3031.

- 776 [49] A. de Palma, M. Ben-Akiva, C. Lefevre, N. Litinas, Stochastic equilibrium model of peak period
 777 traffic congestion, *Transportation Science* 17 (4) (1983) 430–453.
- 778 [50] C. F. Daganzo, Y. Sheffi, On stochastic models of traffic assignment, *Transportation science*
 779 11 (3) (1977) 253–274.
- 780 [51] M. Ben-Akiva, T. Watanatada, Application of a continuous spatial choice logit model, *Structural*
 781 analysis of discrete data with econometric applications (1981) 320–343.
- 782 [52] M. E. Ben-Akiva, S. R. Lerman, *Discrete choice analysis: theory and application to travel*
 783 demand, Vol. 9, MIT press, 1985.
- 784 [53] M. Ben-Akiva, A. De Palma, P. Kanaroglou, Dynamic model of peak period traffic congestion
 785 with elastic arrival rates, *Transportation Science* 20 (3) (1986) 164–181.
- 786 [54] D. McFadden, Econometric models of probabilistic choice, *Structural analysis of discrete data*
 787 with econometric applications 198272 (1981).
- 788 [55] K. Train, A validation test of a disaggregate mode choice model, *Transportation Research* 12 (3)
 789 (1978) 167–174. doi:10.1016/0041-1647(78)90120-X.
- 790 [56] D. Ziemke, K. Nagel, R. Moeckel, Towards an Agent-based, Integrated Land-
 791 use Transport Modeling System, *Procedia Computer Science* 83 (2016) 958–963.
 792 doi:10.1016/j.procs.2016.04.192.
- 793 [57] C. De Gruyter, G. Currie, L. T. Truong, F. Naznin, A meta-analysis and synthesis of pub-
 794 lic transport customer amenity valuation research, *Transport Reviews* 39 (2) (2019) 261–283.
 795 doi:10.1080/01441647.2018.1461708.
- 796 [58] G. Currie, N. Fournier, Valuing public transport customer experience infrastructure—A re-
 797 view of methods and application, *Research in Transportation Economics* 83 (2020) 100961.
 798 doi:10.1016/j.retrec.2020.100961.
- 799 [59] R. E. Stone, Some average distance results, *Transportation Science* 25 (1) (1991) 83–91.
 800 doi:10.1287/trsc.25.1.83.
- 801 [60] N. Fournier, E. J. Gonzales, E. Christofa, Controlling Congestion in a Neighborhood Center for
 802 Ring-Radial and Grid Networks, in: 2019 IEEE Intelligent Transportation Systems Conference
 803 (ITSC), 2019, pp. 950–955. doi:10.1109/ITSC.2019.8917453.
- 804 [61] C. F. Daganzo, N. Geroliminis, An analytical approximation for the macroscopic fundamental
 805 diagram of urban traffic, *Transportation Research Part B: Methodological* 42 (9) (2008) 771–
 806 781. doi:10.1016/j.trb.2008.06.008.
- 807 [62] N. Geroliminis, C. F. Daganzo, Existence of urban-scale macroscopic fundamental diagrams:
 808 Some experimental findings, *Transportation Research Part B* 42 (9) (2008) 759–770.
- 809 [63] W. Liu, N. Geroliminis, Modeling the morning commute for urban networks with cruising-
 810 for-parking: An MFD approach, *Transportation Research Part B: Methodological* 93 (2016)
 811 470–494. doi:10.1016/j.trb.2016.08.004.
- 812 [64] J. Haddad, A. Shraiber, Robust perimeter control design for an urban region, *Transportation*
 813 *Research Part B: Methodological* 68 (2014) 315–332. doi:10.1016/j.trb.2014.06.010.
- 814 [65] E. J. Gonzales, Coordinated pricing for cars and transit in cities with hypercongestion, *Eco-*
 815 *nomics of Transportation* 4 (1-2) (2015) 64–81. doi:10.1016/j.ecotra.2015.04.003.

- 816 [66] K. A. Small, X. Chu, Hypercongestion, Journal of Transport Economics and Policy 37 (1)
817 (2003) 319–352.
- 818 [67] B. Greenshields, J. Bibbins, W. Channing, H. Miller, A study of traffic capacity, in: Highway
819 research board proceedings, Vol. 1935, National Research Council (USA), Highway Research
820 Board, 1935.
- 821 [68] C. Daganzo, Fundamentals of transportation and traffic operations, Vol. 30, Pergamon Oxford,
822 1997.
- 823 [69] N. Geroliminis, N. Zheng, K. Ampountolas, A three-dimensional macroscopic fundamental
824 diagram for mixed bi-modal urban networks, Transportation Research Part C: Emerging
825 Technologies 42 (2014) 168–181. doi:10.1016/j.trc.2014.03.004.
826 URL <https://www.sciencedirect.com/science/article/pii/S0968090X14000709>
827 <https://linkinghub.elsevier.com/retrieve/pii/S0968090X14000709>
- 828 [70] N. Zheng, N. Geroliminis, On the distribution of urban road space for multimodal con-
829 gested networks, Transportation Research Part B: Methodological 57 (2013) 326–341.
830 doi:10.1016/j.trb.2013.06.003.
831 URL <https://www.sciencedirect.com/science/article/pii/S0191261513001021>
832 <https://linkinghub.elsevier.com/retrieve/pii/S0191261513001021>
- 833 [71] A. Loder, L. Ambühl, M. Menendez, K. W. Axhausen, Empirics of multi-modal traffic networks
834 – Using the 3D macroscopic fundamental diagram, Transportation Research Part C: Emerging
835 Technologies 82 (2017) 88–101. doi:10.1016/j.trc.2017.06.009.
- 836 [72] N. Zheng, G. Rérat, N. Geroliminis, Time-dependent area-based pricing for multimodal systems
837 with heterogeneous users in an agent-based environment, Transportation Research Part C:
838 Emerging Technologies 62 (2016) 133–148. doi:https://doi.org/10.1016/j.trc.2015.10.015.
839 URL <https://www.sciencedirect.com/science/article/pii/S0968090X15003745>
- 840 [73] N. Zheng, N. Geroliminis, Modeling and optimization of multimodal urban networks with lim-
841 ited parking and dynamic pricing, Transportation Research Part B: Methodological 83 (2016)
842 36–58. doi:https://doi.org/10.1016/j.trb.2015.10.008.
843 URL <https://www.sciencedirect.com/science/article/pii/S0191261515002234>
- 844 [74] N. Fournier, E. Christofa, E. J. Gonzales, A continuous model for coordinated pricing
845 of mixed access modes to transit, Transportation Research Procedia 38 (2018) 956–976.
846 doi:10.1016/j.trpro.2019.05.049.